Biogeosciences Discuss., 10, 11283–11317, 2013
www.biogeosciences-discuss.net/10/11283/2013/
doi:10.5194/bgd-10-11283-2013

Biogeosciences Discussions
Open Access

High greenhouse gas fluxes from grassland on histic gleysol along soil carbon and drainage gradients

K. Leiber-Sauheitl[1], R. Fuß[1,*], C. Voigt[1,2,*], and A. Freibauer[1,*]

[1]Thünen Institute of Climate-Smart Agriculture, Bundesallee 50, 38116 Braunschweig, Germany
[2]Department of Environmental Science, University of Eastern Finland, P.O. Box 1627, 70211 Kuopio, Finland
[*]The co-authors contributed equally to this work.

Received: 17 June 2013 – Accepted: 27 June 2013 – Published: 9 July 2013

Correspondence to: K. Leiber-Sauheitl (katharina.leiber@ti.bund.de)

Published by Copernicus Publications on behalf of the European Geosciences Union.

Abstract

Drained organic soils are anthropogenic emission hotspots of greenhouse gases (GHGs). Most studies have focused on deep peat soils and on peats with high organic carbon content. In contrast, Histic gleysols are characterized by shallow peat layers, which are left over from peat cutting activities, or by peat mixed with mineral soil. It is unknown whether they emit less GHGs than deep Histosols when drained. We present the annual carbon and GHG balance of grasslands for six sites on nutrient-poor histic gleysols with a shallow (30 cm) histic horizon or mixed with mineral soil in Northern Germany (soil organic carbon concentration (C_{org}) from 9 to 52 %).

The net GHG balance, corrected for carbon export by harvest, was around 4 t CO_2-C-eq. ha^{-1} yr^{-1} on soils with peat layer and little drainage (mean annual water table < 20 cm below surface). The net GHG balance reached 7–9 t CO_2-C-eq. ha^{-1} yr^{-1} on soils with peat layer and deeper drainage (mean annual water table > 20 cm below surface) and on soils with sand mixed into the histic horizon, independent of water table level. GHG emissions from drained histic gleysols (i) were as high as those from deep histosols, (ii) linearly related to water table, (iii) but not affected by C_{org} content of the histic horizon. Ecosystem respiration (R_{eco}) was linearly correlated with water table level even if it was below the histic horizon. The R_{eco} : GPP ratio was 1.5 at all sites, so that we ruled out a major influence of the inter-site variability in vegetation composition on annual net ecosystem exchange (NEE).

The IPCC definition of organic soils includes shallow histic topsoil, unlike most national and international definitions of histosols. Our study confirms that this broader definition is appropriate considering anthropogenic GHG emissions from drained organic soils. Countries currently apply soil maps in national GHG inventories which are likely not to include histic gleysols. The land area with GHG emission hotspots due to drainage is likely to be much higher than anticipated.

Deeply drained histic gleysols are GHG hotspots which have so far been neglected or underestimated. Peat mixing with sand does not mitigate GHG emissions. Our study

implies that rewetting organic soils, including histic gleysols, has a much higher relevance for GHG mitigation strategies than currently recognized.

1 Introduction

Organic soils constitute three percent (Montanarella et al., 2006; Kottek et al., 2006) of the land area of the temperate zone in Europe. A large fraction of them has been drained for forestry, agriculture, and peat extraction. In Germany, organic soils make up approximately five percent of the land area, about 1.7 million ha (UBA, 2012; BÜK 1000, Richter, 1998). Drainage for agricultural purposes or industrial peat extraction was conducted on nearly all of these soils (UBA, 2012). During cultivation of organic soils, degradation of soil organic substances caused emission of high amounts of greenhouse gases as well as subsidence of the peat layers. As a result, only shallow peat soils remain at many former peatland areas and many peatlands even have completely disappeared (e.g. 61 % over 30 yr in Denmark, DCE, 2012).

The loss of peatland areas as carbon storage significantly contributes to global warming (Limpens et al., 2008).

The dominant land use in the boreal zone of Europe is forestry (Drösler et al., 2008), whereas in the temperate zone grassland of varying management intensity predominates (Schrier-Uijl et al., 2010). CO_2 emissions from drained peat scale almost linearly with the depth of the aerated soil above the water table (Dinsmore et al., 2009; Aerts and Ludwig, 1997). Peat substrate quality also influences the amount of GHG emissions since the amount of easily degradable carbon is positively correlated with CO_2, CH_4 and N_2O fluxes (Blodau, 2002).

Most studies focus on peat soils, which meet the definition of histosols. histosols are defined to feature high carbon contents (20 to 30 %) and an organic horizon larger than 40 cm (WRB, 2008). The IPCC definition of peat soils is broader and assumes that also shallow peat soils (≥ 10 cm) and strongly degraded ones (≥ 12 % C_{org}) behave like real peat soils concerning GHG fluxes (IPCC, 2006). Most countries ignore soils

BGD
10, 11283–11317, 2013

with a lower organic carbon content in the national GHG inventory and often focus on profound organic soils. In contrast, in the Danish GHG inventory it is assumed that soils intermediate to typical mineral soils (C_{org} concentration $< 6\,\%$) and peat (C_{org} concentration $> 15\,\%$) emit half as much GHG as organic soils (DCE, 2012). However, according to this report no measurements were conducted on these soils.

To fill this data gap and to test the validity of GHG inventory assumptions, we focus on the most common land-use type in temperate climates (grassland) and measure GHGs along drainage and carbon gradients on a heavily degraded organic soil, which meets the IPCC definition of "organic soil". We test two hypotheses: firstly, GHG emissions (mainly CO_2) of histic gleysols increase linearly with drainage depth in the peat layer and level off when the water table falls below the peat layer. Secondly, peat mixed with mineral subsoil and resulting lower C_{org} concentration emits lower amounts of GHG than unmixed peaty soil with a high C_{org} concentration.

We show, however, that even in shallow histic gleysols and in histic gleysols mixed with mineral soil, GHG emissions remain as high as in deep peat soils and are driven by water table.

2 Material and methods

2.1 Study site Grosses Moor (Great Peat Bog)

The Grosses Moor (Great Peat Bog) (Gifhorn, Germany, 52°34′54.22′′ N, 10°39′46.43′′ E) is a bog-fen peat complex of 6000 ha situated close to the eastern climatic boundary for bog formation. It is located within a former moraine plain from the Saale ice age and the meltwater of the Warthe stage initiated bog formation (Overbeck, 1952). The original ombrotrophic peat bog was altered by peat drainage and peat cutting during the 19th century. As a result, nowadays the Grosses Moor is influenced by groundwater. Mean annual temperature was 8.5 °C and mean annual precipitation was 663 mm in the time period 2008–2011. Mineral substrates below the peat are sandy

BGD
10, 11283–11317, 2013

terraces and partly Pleistocene clay layers. Formerly up to six meter deep peat layers were altered by peat cutting and deep plough cultivation, which created strong small scale heterogeneity. The original bog vegetation has been nearly completely destroyed. Typical vegetation now consists of large cultivated areas, grasslands, and forests of pine and birch as well as purple moor-grass (*Molinia caerulea*), soft rush (*Juncus effusus*) and Erica heath in peat harvest areas. About 2700 ha were turned into restoration areas in 1984. About 2720 ha of abandoned peat cut areas are used as extensive grassland.

The study area is managed as extensive grassland. Sheep graze one to two times a year. Mulching is conducted in autumn. No fertilizer is applied.

The study area is characterized by small peat shoulders and depressions with different water table levels and an irregular anthropogenic mixing of peat layer and mineral soil. Although the entire study area is classified as grassland, the vegetation also shows a gradient from grass dominance to moss dominance.

The small-scale heterogeneity of the study area was surveyed to select sites with diverging soil organic carbon (SOC) concentration in topsoil, C stocks, and water table levels. According to a survey report and own preliminary investigations, two transects (each 310 m) were established at 100 m distance to each other in the area of the field where peat cutting, ploughing, and sand mixing occurred. Every ten meters sampling was carried out by auger until the sandy layer was hit. Auger samples were divided in 0–0.3 m (peat layer) and 0.3–0.6 m (sandy layer). Carbon content of the peat layer was determined by loss on ignition. Six sites were selected in order to achieve similar peat depths (0.25–0.3 m), differing SOC concentrations, and differing water levels. The resulting site characteristics are presented in Table 1. Sites with a C_{org} content below 15 % were classified as C_{low}, > 15 % to 35 % C_{org} as C_{med}, and > 35 % to 55 % C_{org} as C_{high}. Mean groundwater levels W during the study period are indicated by index in centimeters below soil surface. Resulting, sites C_{med} W_{39}, C_{low} W_{29} and C_{low} W_{14} are located on transect 1 within 70 m distance and sites C_{high} W_{11}, C_{high} W_{22} and C_{high}

BGD
10, 11283–11317, 2013

W_{17} on transect 2 within 30 m distance. Sites were fenced to keep off sheep and other animals.

2.2 Measurement of site characteristics

Photosynthetic active radiation (PAR), precipitation, and air temperature were continually measured at a local meteorological station. PAR was manually logged at each site during measurements.

Groundwater levels were continually recorded at each site every 15 min by groundwater data loggers (Mini-diver, Schlumberger). In order to eliminate short-term disturbances, a moving median was calculated over a 75 min window. Subsequently, moving median values were aggregated to one hour values.

Soil temperatures in 0.1, 0.05, 0.02 m were continually logged at each site every 5 min from soil temperature sensors.

Mineral nitrogen (N_{min}) contents of the 0–0.2 m soil layer were analyzed according to VDLUFA (1997) by extraction with 0.01 M $CaCl_2$ at every N_2O measurement. For each site the measured N_{min} values were extrapolated to N_{min} stocks per hectare. The pH values were determined with $CaCl_2$ according to DIN ISO 10390 (HBU, 2005). C_{org} of each site was measured with an elemental analyzer (variomax C, Elementar). Bulk density was measured according to DIN ISO 11272 in 0–0.3 m (HBU, 1998).

Plant species were determined according to Oberdorfer (2001) and species abundance was classified according to the Londo scale (Londo, 1976). Sedge, grass and moss cover was determined for every site.

Green biomass was manually harvested from the plots after each grazing by cutting to 5 cm above the soil surface. At all sites only the grass and sedge biomass was removed; mosses were left untouched. Fresh weight and weight after drying at 60 °C were determined. For carbon and nitrogen measurement (Leco, TruMac CN) a pooled and homogenized sample of all biomass from a plot was used. The C and N values of three replicate plots were averaged per site. C and N contents of the biomass of all cut dates were summed and defined as biomass export of each site.

2.3 GHG flux measurements

CO_2, CH_4, and N_2O fluxes were measured with manual static chambers (Drösler, 2005) at the six sites. Rows of triplicate chamber frames (0.61 m^2, 0.4 m distance between frames) were installed on each site for gas flux measurements. Measurements were conducted at least fortnightly. For CO_2, sites C_{med} W_{39}, C_{low} W_{29} and C_{low} W_{14} and sites C_{high} W_{11}, C_{high} W_{22} and C_{high} W_{17} were measured on the same day, respectively.

The period used for carbon and GHG annual balance was chosen from 1 June 2011 until 1 June 2012.

2.4 CO_2 modelling

Diurnal cycles of CO_2 fluxes were measured with an infrared gas analyzer (LI-820, LI-COR, USA) connected to opaque PVC chambers (for respiration, chamber height 0.5 m, 2 to 5 min chamber closure) and transparent plexiglass chambers (for net ecosystem exchange, chamber height 0.5 m, 1.5 to 3 min chamber closure) (PS-plastic, Eching, Germany).

Fluxes were calculated by linear regression with CO_2-Flux Version 1.0.30 (Beetz et al., 2013). Exclusion criteria of CO_2 fluxes were PAR changes larger than 10 % of the starting value and more than 1.5 °C increase in chamber temperature. Near zero fluxes with small R^2 were not discarded (Alm et al., 2007). A 50 point moving window (measurement frequency 1.3 s) was applied to find fluxes with maximum R^2 and minimum variance, respectively. Both optimization procedures resulted often in identical flux estimates (53 % of all fluxes), but differed in particular during sunrise. Therefore, the mean value of the fluxes from the two optimization procedures was used as a somewhat conservative flux estimate. 19 % of all fluxes had a difference of less than 5 % between the two procedures and 14 % of all fluxes had a difference of more than 20 %. Daily net ecosystem exchange (NEE), ecosystem respiration (R_{eco}), and gross primary production (GPP) were modeled according to Alm et al. (1997), Drösler

(2005), and Beetz et al. (2013) with some adaptations to site conditions as described below.

The annual model was calculated separately for each site. Since the transparent chambers absorb a maximum of five percent of the incoming radiation according to the manufacturer (PS-plastic, Eching, Germany), the PAR-data from the measurement campaigns were corrected by a factor of 0.95. Diurnal cycles of PAR values differed between on-site measurements and measurements at the meteorological station. This was corrected using empirical functions ($\mathrm{PAR} = a \cdot \mathrm{PAR}^{b}_{\mathrm{station}}$), which were derived separately for sites $\mathrm{C_{med}}\ W_{39}$, $\mathrm{C_{low}}\ W_{29}$ and $\mathrm{C_{low}}\ W_{14}$ and sites $\mathrm{C_{high}}\ W_{11}$, $\mathrm{C_{high}}\ W_{22}$ and $\mathrm{C_{high}}\ W_{17}$, respectively, using robust non-linear regression (Rousseeuw et al., 2012; Fig. S1 in the Supplement). The location of the sites and the meteorological station were at different distances from an adjacent tree line, which resulted in different times when direct sunlight reached the PAR sensors at dawn. Since the meteorological station logged every 0.5 h, but the radiation conditions changed at a higher frequency, additional scatter occurred in the data due to clouds and other effects.

The temperature dependent R_{eco} flux model was calculated according to Lloyd-Taylor (1994):

$$R_{\mathrm{eco}} = R_{\mathrm{ref}} \times \exp\left[e_0 \times \left(\frac{1}{T_{\mathrm{ref}} - T_0} - \frac{1}{T - T_0}\right)\right] \quad (1)$$

R_{ref} respiration at the reference Temperature [$\mathrm{CO_2-C\,mg\,m^{-2}\,h^{-1}}$]

e_0 activation energy [K]

T_{ref} reference temperature: 283.15 [K]

T_0 temperature constant for the start of biological processes: 227.13 [K]

The model was fitted to soil temperatures in 0.02 m depth, which resulted in robust fits and was considered to be representative both of plant and of soil respiration. On-site temperatures were used for fitting rather than temperatures from the meteorological

BGD
10, 11283–11317, 2013

station as they resulted in better fit quality. If the observed temperature range during a measurement campaign was too small to model temperature dependency, the campaign was excluded from calibration and only used for validation. To account for management events, e_0 and R_{ref} were kept constant from the preceding measurement campaign until the cut date. After the cut parameters were taken from the subsequent measurement campaign. The annual R_{eco} model was calculated on a 0.5 hourly basis using on-site temperature data.

The PAR dependent NEE flux model was calculated according to Michaelis-Menten (1913) modified by Falge et al. (2001):

$$\mathrm{NEE} = \frac{(\mathrm{GP2000} \times \alpha \times \mathrm{PAR})}{\left(\mathrm{GP2000} + \alpha \times \mathrm{PAR} - \frac{\mathrm{GP2000}}{2000} \times \mathrm{PAR}\right)} + R_{eco} \quad (2)$$

GP2000	rate of carbon fixation at PAR 2000 [$CO_2 - \mathrm{C\,mg\,m^{-2}\,h^{-1}}$]
PAR	photon flux density of the photosynthetic active radiation [$\mathrm{W\,m^{-2}}$]
α	initial slope of the curve; light use efficiency [$CO_2 - \mathrm{C\,mg\,m^{-2}\,h^{-1}/W\,m^{-2}}$]

PAR values used for fitting were again on-site values. Biomass cuts were included in the NEE model by applying α and GP2000 from the preceding measurement campaign until the cut date and setting α to −0.01 and GP2000 to −4 after the cut according to observations on other grassland sites (Drösler et al., 2013). NEE values were modeled using corrected PAR values from the meteorological station. In the end GPP was calculated on a 0.5 hourly basis:

$$\mathrm{GPP} = \mathrm{NEE} - R_{eco} \quad (3)$$

Values between two measurement campaigns were calculated separately using the campaign results on both sides, and then taken as the distance weighted mean of both values.

BGD
10, 11283–11317, 2013

2.5 CH_4 and N_2O annual calculations

Opaque PVC chambers were used for CH_4 and N_2O flux measurements (PS-plastic, Eching, Germany). Chamber air samples were collected in headspace vials 0, 20, 40, and 60 min after chamber closure. Measurements were carried out with a Varian CP-3800 GC-FID/-ECD using a headspace autosampler (QUMA Elektronik and Analytik GmbH, Germany).

The following algorithm was used to calculate fluxes:

1. Flux rates were calculated using ordinary linear regression, robust linear regression (Huber, 1981), and Hutchinson–Mosier regression (HMR; Pedersen et al., 2010).

2. For the standard case of 4 data points the flux calculated by robust linear regression was used per default. Only if the following conditions were met, the non-linear flux estimation (HMR) was used instead:

   (a) the HMR function could be fitted,

   (b) Akaike information criterion (AIC; Burnham and Anderson, 2004) was smaller for HMR fit than for linear fit,

   (c) p value of flux calculated using HMR was smaller than that from robust linear fit,

   (d) and the flux calculated using HMR was not more than 4 times the flux from robust linear regression. This avoided severe overestimation of fluxes.

3. Ordinary linear regression was applied for three data points. If less than three data points were available (due to loss of samples) no flux was calculated and the measurement discarded.

As a result 27 % of all CH_4 fluxes and 16 % of all N_2O fluxes were calculated non-linearly. Depicting square roots of the flux standard error in boxplots and histograms showed distributions relatively similar to normal distribution. Some extreme values were detected. Associated flux values were considered carefully as potential outliers based on field and lab notes as well as the pattern of CO_2 concentrations. If the third or last CO_2 concentration was not plausible, e.g., lower than the previous one, the sample was deleted and linear regression applied. If an outlier occurred with CH_4 and N_2O fluxes and not with CO_2, values were not corrected since CH_4 and N_2O were often near ambient or near zero fluxes occurred.

The square root of the flux standard error of all measured fluxes followed a normal-like distribution with a median of $0.11\sqrt{\mathrm{mg CH_4-C\,m^{-2}\,h^{-1}}}$ for CH_4 and $1.75\sqrt{\mathrm{\mu g N_2O-N\,m^{-2}\,h^{-1}}}$ for N_2O which demonstrates a sufficient accuracy of the flux measurements.

2.6 Statistical analyses

R 2.15.2 (R Core Team, 2012) was used for statistics and modeling. In particular, package *nlme* (package version 3.1.108; Pinheiro et al., 2013) was used for linear mixed-effects models.

For error estimation of the CO_2 fluxes (NEE, GPP, R_{eco}) and to construct a confidence interval for the annual NEE, GPP and R_{eco} fluxes a Monte Carlo simulation was conducted for each site as follows:

1. The robust fit of the PAR correction function was performed 1000 times with bootstrap resamples of the PAR data points (on-site/station).

2. From the R_{eco} fits of all measurement campaigns bootstrap parameter samples were created using bootstrap of the residuals (Efron, 1979). Bootstrap of the residuals preserves the distribution of x values, which is particularly important for small data size. The bootstrap sample size was again 1000, but bootstrap fits were discarded if they did not successfully model a temperature dependence ($e_0 = 0$). On average 70 % of the fits were successful. Using these, about 700 annual R_{eco}

models were calculated for each site. The medians of these models were in excellent agreement with the original models. 97.5 % and 2.5 % quantiles at each time point were used to construct confidence intervals of the time series. Confidence intervals of the annual sums were constructed in the same way.

3. Each R_{eco} bootstrap fit was paired with a PAR correction bootstrap fit and based on these the NEE models were refitted for each site and measurement campaign. With these NEE fits, bootstrap of the residuals was conducted as described above. Again only successful fits (52 % on average) were used. The high number of failed fits results from the strong non-linearity of the NEE model and the relatively low number of data points at each measurement campaign. About 364 000 (700 × 520) annual models were calculated from the bootstrap parameter samples and confidence intervals constructed as described before.

3 Results

3.1 Driver variables

In the investigation period, daily mean value of the air temperature ranged from −14.8 to 23.5 °C and the 0.02 m soil temperatures were between −1.6 °C and 20.7 °C. Daily mean air temperature was below zero degrees Celsius during 27 days, while this was the case for soil temperature on 11 days (Fig. 1). A longer period of snow cover occurred during February 2012.

Groundwater levels (GWL) were within the peat layer at each site during different periods. At the driest sites (C_{med} W_{39} and C_{low} W_{29}) GWLs were in the peat layer for 128 and 214 days, respectively. In contrast, sites C_{low} W_{14}, C_{high} W_{22} and C_{high} W_{17} had a similar number of days with high water levels (304, 271 and 273, respectively) whereas at the wettest site (C_{high} W_{11}) water levels were within the peat layer for the whole year. Groundwater levels above the surface occurred only on the wet sites (C_{low} W_{14}, C_{high} W_{11}, and C_{high} W_{17}) during 83, 34, and 35 days, respectively. Longer periods

BGD
10, 11283–11317, 2013

of water saturation were observed on these sites during the winter season, whereas during the summer season few precipitation events caused short periods of flooding. Site C_{high} W_{11} showed the lowest groundwater level dynamics whereas site C_{med} W_{39} had the highest groundwater level dynamics of all sites (Fig. S2 in the Supplement).

Mineral nitrogen stock was low on all sites (Table 1). The maximum value of $17\,kg\,ha^{-1}$ was found at site C_{low} W_{29} with the highest plant biomass, whereas the moss-dominated sites C_{high} W_{11}, C_{high} W_{22} and C_{high} W_{17} contained the smallest N_{min} stocks of $2\,kg\,ha^{-1}$. The N_{min} differences between the sites were also reflected in vegetation composition and biomass amounts.

Plant species composition and vegetation cover were similar within one site whereas vegetation showed clear differences between the single sites (Table 2). Sites where the histic horizon was mixed with sand, or the mean annual water table was below about 20 cm, had high abundance of grasses and moderate productivity. Sphagnum and other mosses were present on sites with high C_{org} and little drainage, where productivity was low. In detail, C_{med} W_{39}, C_{low} W_{29} and C_{low} W_{14} were dominated by sedges and grasses in different levels and without any moss occurrence, which is also reflected in the highest biomass exports (1.7 to $2.9\,t\,ha^{-1}\,a^{-1}$; three grazing events and one mulching event) in comparison to the other sites. In contrast, C_{high} W_{11}, C_{high} W_{22} and C_{high} W_{17} had high moss abundance and a lower grass and sedge biomass. The biomass export on these sites was only in the range of 0.3 to $0.6\,t\,ha^{-1}\,a^{-1}$ during one grazing and one mulching event.

3.2 CO_2

Gross primary production on sites C_{med} W_{39}, C_{low} W_{29} and C_{low} W_{14} was about $12\,t\,C\,ha^{-1}\,a^{-1}$, whereas on sites C_{high} W_{11}, C_{high} W_{22} and C_{high} W_{17} GPP was about $6\,t\,C\,ha^{-1}\,a^{-1}$ (Table 3), reflecting the difference of biomass productivity and nitrogen content between the different sites (Tables 2 and 1).

BGD
10, 11283–11317, 2013

During the vegetation period plant growth influenced NEE budgets of all sites, which as a result became CO_2 sinks as well as CO_2 sources over the course of the year (especially right after grazing). From October until March NEE fluxes were on a low level on all sites and they were dominated by R_{eco} since GPP was near zero on all sites.

C_{med} W_{39}, C_{low} W_{29} and C_{low} W_{14} showed a similar time series (Fig. 2). However, in spring and summer GPP gradually decreased from C_{low} W_{29} to C_{med} W_{39} and C_{low} W_{14}. This is in line with the productivity differences of grass and sedge species on the respective sites. C_{high} W_{11}, C_{high} W_{22} and C_{high} W_{17} also feature similar time series. Though in spring and summer GPP of site C_{high} W_{22} was larger than on sites C_{high} W_{17} and C_{high} W_{11}, these three sites had nearly identical annual GPP fluxes. GPP is in line with the different productivity of grass and sedge vs. moss species (Table 2).

Ecosystem respiration of sites C_{med} W_{39}, C_{low} W_{29} and C_{low} W_{14} (about $18\,\mathrm{t\,C\,ha^{-1}\,a^{-1}}$) was nearly twice as high as of sites C_{high} W_{11}, C_{high} W_{22} and C_{high} W_{17} ($10\,\mathrm{t\,C\,ha^{-1}\,a^{-1}}$). This again reflects the vegetation differences. The same trends were found between the sites as before for GPP. This leads to the assumption that plant respiration was dominating R_{eco} differences between the sites, which is confirmed by highly significant correlations between daily mean values of GPP and R_{eco} for each site ($p < 2.2 \times 10^{-16}$).

All of the sites in the Grosses Moor were both source and sink of CO_2 at different times with some clear annual NEE trends (Fig. 2). C_{med} W_{39}, C_{low} W_{29} and C_{low} W_{14} exhibited NEE values of about $5\,\mathrm{t\,C\,ha^{-1}\,a^{-1}}$ whereas sites C_{high} W_{11} and C_{high} W_{17} had a NEE of about $3\,\mathrm{t\,C\,ha^{-1}\,a^{-1}}$ only (Fig. 3). NEE of site C_{high} W_{22} was between the two groups. Differences between sites in annual NEE were less prominent than for GPP and R_{eco}. Grass dominated sites, the sites with higher plant productivity, exhibited higher NEE fluxes than sites containing predominantly mosses. However, low NEE fluxes occurred on all sites during the winter season because grasses were cut in autumn.

BGD
10, 11283–11317, 2013

3.3 CH_4

CH_4 fluxes were on a low level with highest CH_4 emissions on site C_{high} W_{17} whereas site C_{low} W_{29} emitted the lowest amounts of CH_4 (Table 3) reflecting water level differences. Annual fluxes ranged from 1.1 to 29.8 kg C ha^{-1} a^{-1} and therefore all sites represented small sources.

Strongest CH_4 emissions occurred during periods with high water levels and warm temperatures.

3.4 N_2O

Only near zero N_2O fluxes occurred on any site. Annual fluxes ranged from −0.3 kg N_2O-N ha^{-1} a^{-1} to 0.05 kg N_2O-N ha^{-1} a^{-1} and were not significant.

3.5 Annual C and GHG balance

Including the carbon from vegetation export (Table 2) and from CH_4 emissions (Table 3), the annual carbon balance of the sites was in the range from 3.1 to 8.2 t C ha^{-1} a^{-1} (Table 4, GWP-C balance).

Differences in the amount of exported carbon altered the ranking of sites according to their annual carbon and greenhouse gas balance compared to their NEE ranking. Sites C_{low} W_{29} and C_{med} W_{39} emitted more GHGs than site C_{low} W_{14}. This indicates that higher productive sites emitted more GHGs. More distinct differences between the sites became apparent this way than if NEE was considered in isolation. The ranking of the sites according to their GHG balance did not change if N_2O emissions were included (Table 4).

BGD
10, 11283–11317, 2013

4 Discussion

4.1 Magnitude of GHG fluxes

The CO_2 fluxes of the Grosses Moor are within the range of other studies in comparable German peatlands (e.g. Drösler, 2005) as well as in peatlands of northern latitudes (e.g. Alm et al., 1997; Bellisario et al., 1998). Similar NEE fluxes and biomass export were observed on drained permanent grassland in Denmark (Elsgaard et al., 2012). In comparison to further German grassland sites on organic soils, emissions of the Grosses Moor are in the upper range of all considered GHG balances (Fig. 4; Drösler et al., 2013).

Low CH_4 emissions similar to those from the dry sites (C_{med} W_{39} and C_{low} W_{29}) were reported by Drösler (2005) for a dry, peat cut heath. The two sites with the highest fluxes (C_{high} W_{11} and C_{high} W_{17}) are in the lower third of average emission rates of 5–80 mg CH_4-C m^{-2} d^{-1} given by Blodau (2002) for natural peatlands. Comparable low CH_4 fluxes were found in three drained Danish peatlands, increasing with higher cover of plants with aerenchymatic tissues (Schäfer et al., 2012). Also in the Grosses Moor, sites with a higher cover of sedges (Table 3) emitted more CH_4. Because of their aerenchymatic tissue, which channels CH_4 fluxes from soil, sedges prevent CH_4 from further oxidation by soil microbes (Thomas et al., 1996). Low water levels during warm periods can result in oxidation of CH_4 by methanothrophic bacteria to CO_2 in the aerated soil zone, thereby increasing respiration (Lai, 2009). According to Blodau (2002) large root density can increase CH_4 oxidation which results in low CH_4 emissions rates at the soil surface. In soils with C/N ratios above 25 (Table 1), low CH_4 emissions can be expected (Klemedtsson et al., 2005). The CH_4 emission patterns observed at the Grosses Moor confirm these mechanisms.

Low N_2O values as in the Grosses Moor were reported for a dry peat cutting area by Drösler (2005). Other drained peatlands with permanent grass cover but more profound

BGD
10, 11283–11317, 2013

peat layer emitted larger amounts of N_2O (Petersen et al., 2012). The Grosses Moor reacts like nutrient-poor bogs with regard to N_2O.

4.2 Precision of the annual CO_2 budget

Our error analysis is based in principle on the bootstrap approach and error propagation using Monte-Carlo simulation. Resulting confidence intervals, which include measurement error as well as on-site heterogeneity, were overall relatively narrow. However, the interpolation between the measurement campaigns could constitute a significant additional source of error. The calibration of temperature and PAR models by frequent campaigns captures effects of changing water table and biomass. But for interpolation between campaigns we assume a linear change from one calibration to the next one. With the available data it was not possible to quantify the interpolation error in the error analysis. The interpolation error could be quantified by very frequent measurement campaigns with automated chambers. We used measurement campaigns, which did not result in adequate model fits, for validating the interpolation. The CO_2 fluxes of the validation campaigns were well described by the models so that we can conclude that the interpolation is robust.

Most of the CO_2 measurement campaigns covered the full range of temperature and radiation for the interpolation so that the model error remained low for most of the time and the method was robustly applied. There were few periods (< 5 days in summer and < 47 days in winter) for which temperature was continuously outside the temperature range of at least one of the adjacent campaign days. These periods are characterized by higher model uncertainty due to extrapolation of the R_{eco} fits (Fig. 2).

Our NEE error estimates (about ±0.4 $\mathrm{Mg\,C\,ha^{-1}\,yr^{-1}}$) without interpolation error were at the low end of error estimates for eddy covariance measurements, for which errors in the range of ±0.3 to ±1.8 $\mathrm{Mg\,C\,ha^{-1}\,yr^{-1}}$ (Woodward and Lomas, 2004) or higher (Kruijt et al., 2004) have been reported. We expect that the error of the chamber based approach with interpolation error is likely to be comparable with eddy covariance. Thus,

BGD
10, 11283–11317, 2013

High greenhouse gas fluxes from grassland on histic gleysol

K. Leiber-Sauheitl et al.

the chamber technique with model-based CO_2 flux interpolation is a reliable method for studying small-scale heterogeneity and sites where eddy covariance is not applicable.

4.3 C_{org} effects

The GHG fluxes of the histic grasslands of the Grosses Moor are in the upper range of German managed grassland sites on organic soils with deep peat layers (Fig. 4; Drösler et al., 2013). This is opposite to our expectation of lower GHG emissions from soil with shallow histic layers, in which less soil organic carbon is exposed to mineralization by drainage than in soils with deep peat layers. Obviously, the substrate quality and decomposition level of the peat play a larger role on emission rates (Berglund and Berglund, 2011) than peat depth.

We defined the effective C stock as the fraction of aerated carbon in the soil profile. Effective C stock showed no effect on GHG emissions. Moreover no significant correlation was found between C_{org} concentration in the topsoil and GHG emissions (Fig. 5a).

All sites exhibited highly degraded (H10 on the Van-Post scale; AG Boden, 2005), amorphous organic material in the peat layer (0 to 0.3 m). The sand intermixture (C_{med} W_{39}, C_{low} W_{29} and C_{low} W_{14}) resulted in yield increase via harvested biomass (Table 2) instead of C_{org} stabilization on the mineral phase. We therefore reject our hypothesis that peat mixed with mineral subsoil and resulting lower C_{org} concentration emits lower amounts of GHG than unmixed peat soil with a high C_{org} concentration.

Mixing peat with sand has been a widespread soil management practice to improve the suitability of peat soils for agriculture (Göttlich, 1990) and is still practiced today. Our findings suggest that peat mixing does not mitigate GHG emissions from high organic carbon soils.

This finding has serious consequences for regional to national GHG balances because histic gleysols are relatively widespread. Due to a lack of data, shallow or mixed organic soils such as histic gleysols, which do not fall under the definition of histosols but do fall under the definition of organic soils of IPCC (IPCC, 2006), tended to be neglected as source of GHGs in national GHG inventories under the UNFCCC or estimated to emit half of the annual CO_2 emissions of real histosols (DCE, 2012). Adding histic gleysols to the histosol area, the land area with GHG emission hotspots due to drainage is likely to be much larger than anticipated.

4.4 Water level effects

The variation between measurement campaigns showed that GPP was not significantly influenced by water levels but mainly by radiation. This was also reported by Lindroth et al. (2007).

Water levels had a strong influence on R_{eco} fluxes ($p = 0.0004$, correlation between both: $R^2 = 0.91$; Fig. 6) as analyzed by a linear mixed-effect model (Table S1 in the Supplement). A strong correlation between water table and CO_2 emissions was also observed by Silvola et al. (1996) and Berglund and Berglund (2011).

Annual NEE budgets were positively correlated to mean annual water table levels (Fig. 5b).

Peat mineralization generally increases linearly when the water table lowers (Dinsmore et al., 2009; Aerts and Ludwig, 1997). Our study confirms this rule on a daily (Fig. 6) and annual (Fig. 5b) time scale. This increase in heterotrophic respiration may level off in dry conditions when the water table falls below the peat layer, and little extra SOC from deeper soil is exposed to aerobic conditions. On our sites, however, there was no significant difference in the relation between R_{eco} and water table when water levels were in the peat or the in subjacent sand layer. Only the water table level and the depth of the aerated soil zone affected R_{eco} but not the effective aerobic SOC stock although water table sometimes dropped to −30 cm below the peat layer. Consequently, peat mineralization seems to be driven by soil moisture in the topsoil rather than by peat layer depth. Deeper water levels result in drier topsoil, which is hence faster mineralized.

BGD
10, 11283–11317, 2013

We confirm our hypothesis that GHG emissions of histic gleysols (mainly CO_2) increase linearly with drainage depth but reject our hypothesis that CO_2 emissions level off when the water table falls below the peat layer.

Histic gleysols are frequently subject to deep drainage for agriculture. Histic gleysols tend to be more intensively used for agriculture than histosols due to more suitable soil physical and chemical properties. Our study suggests that deeply drained histic gleysols could be much stronger sources of GHGs than expected.

4.5 Vegetation effects

Differences in vegetation composition and biomass amounts were reflected in GPP amounts (Fig. 2). R_{eco} is not only affected by temperature, which is very similar for all sites, but also by plant biomass, which differs between sites. However, since the ratio of the annual R_{eco} to GPP was almost the same on all sites (mean value of 1.5 ± 0.07; Table 3), the influence of the vegetation on NEE of the different sites can be ruled out.

The C balance of all sites was clearly affected by harvest/grazing. Carbon export was as important as NEE for the annual C balance, especially on sites with high grass biomass (up to 30 % of the C balance for site C_{low} W_{29}). In Danish permanent grassland sites, yield export had a similar contribution to the C balance as in the Grosses Moor (Elsgaard et al., 2012).

5 Conclusions

We showed that GHG emissions of histic gleysols (mainly CO_2) increase linearly with drainage depth and do not level off when the water table falls below the peat level. Drained histic gleysols are GHG hotspots, which have so far been neglected or underestimated.

Grasslands on histic gleysols emit as many GHGs as grasslands on histosols. This confirms the wide definition of organic soils for use in GHG emission inventories by

BGD
10, 11283–11317, 2013

IPCC (IPCC, 2006). Since shallow histic gleysols emit as much CO_2 as deep peat soils, they should be integrated in the national and international definitions of histosols in terms of climate relevant carbon sources.

Peat mixed with mineral subsoil and C_{org} concentration around 10 % emits as much GHG as unmixed peat soil (> 30 % C_{org}). This implies that peat mixing with underlying sand is not a GHG mitigation option.

Supplementary material related to this article is available online at: http://www.biogeosciences-discuss.net/10/11283/2013/ bgd-10-11283-2013-supplement.zip.

Acknowledgements. The joint research project "Organic soils" funded by the Thünen Institute and its twelve participating research institutes aims at closing the data gap by monitoring emissions from eleven catchments in Germany. Various peatlands, differing in preservation and utilization, are investigated in order to derive specific emission factors.

HU Berlin, especially N. Rosskopf, for soil identification and soil properties. M. Hunziger and D. Olbrich for help during the measurement campaigns and in the lab. K. Gilke, R. Lausch, A. Oehns-Rittgerodt for laboratory assistance. S. Belting for plant species knowledge. DWD for climate data of stations Braunschweig, Uelzen, Wittingen-Vorhop and Wolfsburg (Südwest). Schäferei Paulus and Herr Horny for research permission. The peat group of the Thünen Institute of Climate-Smart Agriculture (B. Tiemeyer, E. Frahm, U. Dettmann, S. Frank, M. Bechtold, T. Leppelt) for discussion.

References

Aerts, R. and Ludwig, F.: Water-table changes and nutritional status affect trace gas emissions from laboratory columns of peatland soils, Soil Biol. Biochem., 29, 1691–1698, 1997.

AG Boden: Bodenkundliche Kartieranleitung (Soil survey manual), 5th Edn., Bundesanstalt für Geowissenschaften und Rohstoffe in Zusammenarbeit mit den Staatlichen Geologischen Diensten, Hannover, 2005.

Alm, J., Talanov, A., Saarnio, S., Silvola, J., Ikkonen, E., Aaltonen, H., Nykanen, H., and Martikainen, P. J.: Reconstruction of the carbon balance for microsites in a boreal oligotrophic pine fen, Finland, Oecologia, 110, 423–431, 1997.

Alm, J., Shurpali, N. J., Tuittila, E.-S., Laurila, T., Maljanen, M., Saarnio, S., and Minkkinen, K.: Methods for determining emission factors for the use of peat and peatlands – flux measurements and modelling, Boreal Environ. Res., 12, 85–100, 2007.

Beetz, S., Liebersbach, H., Glatzel, S., Jurasinski, G., Buczko, U., and Höper, H.: Effects of land use intensity on the full greenhouse gas balance in an Atlantic peat bog, Biogeosciences, 10, 1067–1082, doi:10.5194/bg-10-1067-2013, 2013.

Bellisario, L. M., Moore, T. R., and Bubier, J. L.: Net ecosystem CO_2 exchange in a boreal peatland, northern Manitoba, Ecoscience, 5, 534–541, 1998.

Berglund, O. and Berglund, K.: Influence of water table level and soil properties on emissions of greenhouse gases from cultivated peat soil, Soil Biol. Biochem., 43, 923–931, 2011.

Blodau, C.: Carbon cycling in peatlands: a review of processes and controls, Environ. Rev., 10, 111–134, 2002.

Burnham, K. P. and Anderson, D. R.: Multimodel inference: understanding AIC and BIC in model selection, Sociol. Method. Res., 33, 261–304, 2004.

DCE: Scientific Report from DCE – Danish Centre for Environment and Energy No. 19, Emission Inventories 1990–2010 – submitted under the United Nations Framework Convention on Climate Change and the Kyoto Protocol, 2012.

Dinsmore, K. J., Skiba, U. M., Billett, M. F., and Rees, R. M.: Effect of water table on greenhouse gas emissions from peatland mesocosms, Plant Soil, 318, 229–242, 2009.

Drösler, M.: Trace Gas Exchange and Climatic Relevance of Bog Ecosystems, Southern Germany, Lehrstuhl für Vegetationsökologie, Departement Ökologie, TUM, München, 179 pp., 2005.

Drösler, M., Freibauer, A., Christensen, T. R., and Friborg, T.: Observations and status of peatland greenhouse gas emissions in Europe, in: The Continental-Scale Greenhouse Gas Balance of Europe, edited by: Dolman, A. J., Freibauer, A., and Valentini, R., Springer, New York, 243–261, 2008.

Drösler, M., Adelmann, W., Augustin, J., Bergmann, L., Beyer, C., Chojnicki, B., Förster, C., Freibauer, A., Giebels, M., Görlitz, S., Höper, H., Kantelhardt, J., Liebersbach, H., Hahn-Schöfl, M., Minke, M., Petschow, U., Pfadenhauer, J., Schaller, L., Schägner, P., Sommer, M., Thuille, A., and Wehrhan, M.: Klimaschutz durch Moorschutz, Schlussbericht des Vorhabens

"Klimaschutz –Moorschutzstrategien" 2006–2010, Technische Informationsbibliothek u. Universitätsbibliothek, Freising, 2013.

Efron, B.: Bootstrap methods: another look at the jackknife, Ann. Statist., 7, 1–26, 1979.

Elsgaard, L., Gorres, C.-M., Hoffmann, C. C., Blicher-Mathiesen, G., Schelde, K., and Petersen, S. O.: Net ecosystem exchange of CO_2 and carbon balance for eight temperate organic soils under agricultural management, Agr. Ecosyst. Environ., 162, 52–67, 2012.

Falge, E., Baldocchi, D., Olson, R., Anthoni, P., Aubinet, M., Bernhofer, C., Burba, G., Ceulemans, R., Clement, R., Dolman, H., Granier, A., Gross, P., Grunwald, T., Hollinger, D., Jensen, N. O., Katul, G., Keronen, P., Kowalski, A., Lai, C. T., Law, B. E., Meyers, T., Moncrieff, H., Moors, E., Munger, J. W., Pilegaard, K., Rannik, U., Rebmann, C., Suyker, A., Tenhunen, J., Tu, K., Verma, S., Vesala, T., Wilson, K., and Wofsy, S.: Gap filling strategies for defensible annual sums of net ecosystem exchange, Agr. Forest Meteorol., 107, 43–69, 2001.

Göttlich, K.: Moor- und Torfkunde (Peatland and Peat Knowledge), E. Schweizerbart'sche Verlagsbuchhandlung (Nägele und Obermiller), Stuttgart, 1990.

HBU, Hand Book of Soil Analyses (HBU): Soil Quality – Determination of Dry Bulk Density, Beuth Verlag GmbH, Berlin, ISO 11272, 10 pp., 1998.

HBU, Hand Book of Soil Analyses (HBU): Soil Quality – Determination of pH, Beuth Verlag GmbH, Berlin, ISO 10390: 9 pp., 2005.

Huber, P. J.: Robust Statistics, J. Wiley, New York, 1981.

IPCC: 2006 IPCC Guidelines for National Greenhouse Gas Inventories, chapt. 3, Consistent Representation of Lands, Prepared by the National Greenhouse Gas Inventories Programme, edited by: Eggleston, H. S., Buendia, L., Miwa, K., Ngara, T., and Tanabe, K., published: IGES, Japan, 2006.

IPCC: IPCC Fourth Assessment Report (AR4), Cambridge, UK and New York, NY, USA, 996 pp., 2007.

Klemedtsson, L., von Arnold, K., Weslien, P., and Gundersen, P.: Soil CN ratio as a scalar parameter to predict nitrous oxide emissions, Glob. Change Biol., 11, 1142–1147, 2005.

Kottek, M., Grieser, J., Beck, C., Rudolf, B., and Rubel, F.: World map of the Köppen–Geiger climate classification updated, Meteorol. Z., 15, 259–263, 2006.

Kruijt, B., Elbers, J. A., von Randow, C., Araujo, A. C., Oliveira, P. J., Culf, A., Manzi, A. O., Nobre, A. D., Kabat, P., and Moors, E. J.: The robustness of eddy correlation fluxes for Amazon rain forest conditions, Ecol. Appl., 14, S101–S113, 2004.

BGD

10, 11283–11317, 2013

Lai, D. Y. F.: Methane dynamics in northern peatlands: a review, Pedosphere, 19, 409–421, 2009.

Limpens, J., Berendse, F., Blodau, C., Canadell, J. G., Freeman, C., Holden, J., Roulet, N., Rydin, H., and Schaepman-Strub, G.: Peatlands and the carbon cycle: from local processes to global implications – a synthesis, Biogeosciences, 5, 1475–1491, doi:10.5194/bg-5-1475-2008, 2008.

Lindroth, A., Lund, M., Nilsson, M., Aurela, M., Christensen, T. R., Laurila, T., Rinne, J., Riutta, T., Sagerfors, J., Stroem, L., Tuovinen, J.-P., and Vesala, T.: Environmental controls on the CO_2 exchange in north European mires, Tellus B, 59, 812–825, 2007.

Lloyd, J. and Taylor, J. A.: On the temperature dependence of soil respiration, Funct. Ecol., 8, 315–323, 1994.

Londo, G.: Decimal scale for releves of permanent quadrats, Vegetatio, 33, 61–64, 1976.

Menten, L. and Michaelis, M. I.: Die Kinetik der Invertinwirkung, Biochem. Z., 49, 333–369, 1913.

Montanarella, L., Jones, R. J. A., and Hiederer, R.: The distribution of peatland in Europe, Mires and Peat, 1, 1–11, 2006.

Oberdorfer, E.: Pflanzensoziologische Exkursionsflora für Deutschland und angrenzende Gebiete, 8. Aufl., Verlag Eugen Ulmer, Stuttgart, 2001.

Overbeck, F.: Das Große Moor bei Gifhorn im Wechsel hygrokliner und xerokliner Phasen der nordwestdeutschen Hochmoorentwicklung, (The "Großes Moor" near Gifhorn during the alternation of hygrocline and xerocline periods of the northwestern German peat bog development), Walter Dorn Verlag, Bremen, 1952.

Pedersen, A. R., Petersen, S. O., and Schelde, K.: A comprehensive approach to soil-atmosphere trace-gas flux estimation with static chambers, Eur. J. Soil Sci., 61, 888–902, 2010.

Petersen, S. O., Hoffmann, C. C., Schäfer, C.-M., Blicher-Mathiesen, G., Elsgaard, L., Kristensen, K., Larsen, S. E., Torp, S. B., and Greve, M. H.: Annual emissions of CH_4 and N_2O, and ecosystem respiration, from eight organic soils in Western Denmark managed by agriculture, Biogeosciences, 9, 403–422, doi:10.5194/bg-9-403-2012, 2012.

Pinheiro, J., Bates, D., DebRoy, S., Sarkar, D., and R Development Core Team: Linear and Nonlinear Mixed Effect Models, R Package Version 3.1–108., http://cran.r-project.org/web/packages/nlme/index.html, (last access: 21 March 2013), 2013.

BGD

10, 11283–11317, 2013

High greenhouse gas fluxes from grassland on histic gleysol

K. Leiber-Sauheitl et al.

R Core Team: R: A Language and Environment for Statistical Computing, available at: http://www.r-project.org/, (last access: 24 April 2013), 2012.
Richter, A.: Bodenübersichtskarte der Bundesrepublik Deutschland – BÜK 1000 (Soil Survey Map), 2. Aufl., Bundesanstalt für Geowissenschaften und Rohstoffe (BGR), Hannover, 1998.
Rousseeuw, P., Croux, C., Todorov, V., Ruckstuhl, A., Salibian-Barrera, M., Verbeke, T., Koller, M., and Maechler, M.: robustbase: Basic Robust Statistics, R Package Version 0.9–4., available at: http://CRAN.R-project.org/package=robustbase, (last access: 24 April 2013), 2012.
Schäfer, C. M., Elsgaard, L., Hoffmann, C. C., and Petersen, S. O.: Seasonal methane dynamics in three temperate grassland s on peat, Plant Soil, 357, 339–353, 2012.
Schrier-Uijl, A. P., Kroon, P. S., Hensen, A., Leffelaar, P. A., Berendse, F., and Veenendaal, E. M.: Comparison of chamber and eddy covariance-based CO_2 and CH_4 emission estimates in a heterogeneous grass ecosystem on peat, Agr. Forest Meteorol., 150, 825–831, 2010.
Silvola, J., Alm, J., Ahlholm, U., Nykanen, H., and Martikainen, P. J.: CO_2 fluxes from peat in boreal mires under varying temperature and moisture conditions, J. Ecol., 84, 219–228, doi:10.2307/2261357, 1996.
Thomas, K. L., Benstead, J., Davies, K. L., and Lloyd, D.: Role of wetland plants in the diurnal control of CH_4 and CO_2 fluxes in peat, Soil Biol. Biochem., 28, 17–23, doi:10.1016/0038-0717(95)00103-4, 1996.
UBA: National Inventory Report for the German Greenhouse Gas Inventory 1990–2010, Submission under the United Nations Framework Convention on Climate Change and the Kyoto Protocol 2012, Dessau, Germany, 2012.
VDLUFA: Bestimmung von mineralischem (Nitrat-)Stickstoff in Bodenprofilen (Nmin-Labormethode), in: Methodenbuch Teil 2, edited by: VDLUFA, Speyer, Germany, 1997.
Woodward, F. I. and Lomas, M. R.: Vegetation dynamics – simulating responses to climatic change, Biol. Rev., 79, 643–670, 2004.
WRB: World Reference Base for Soil Resources 2006. Ein Rahmen für internationale Klassifikation, Korrelation und Kommunikation, Deutsche Ausgabe, Bundesanstalt für Geowissenschaften und Rohstoffe, Hannover, 2008.

Table 1. Site characterization.

Site	Soil class (WRB)	C_{org} [%][a]	C stock [kg m^{-2}][a]	Bulk density [g cm^{-3}][a]	C/N[a]	N_{min} [kg ha^{-1}][b]	pH ($CaCl_2$)	Mean WTL [m][c]
C_{med} W_{39}	histic gleysol	34.3	46	0.54	29	6	3.8	0.39
C_{low} W_{29}	mollic gleysol drainic	11.3	36	1.06	27	17	4.5	0.29
C_{low} W_{14}	mollic gleysol drainic	9.3	29	0.97	24	10	4.5	0.14
C_{high} W_{11}	histic gleysol drainic	51.7	71	0.45	28	2	4.1	0.11
C_{high} W_{22}	histic gleysol drainic	47.7	41	0.29	28	2	3.8	0.22
C_{high} W_{17}	histic gleysol drainic	47.7	41	0.29	28	2	3.8	0.17

C = carbon.
W = mean annual water table.
[a] organic carbon, C stock, C/N and bulk density in 0–30 cm.
[b] mineral nitrogen in 0–20 cm in the time interval 1 June 2011 to 1 June 2012.
[c] WTL = water table level in the time interval 1 June 2011 to 1 June 2012.

BGD
10, 11283–11317, 2013

Table 2. Biomass export from sites (1 June 2011 to 1 June 2012; site mean value ± one stand ard deviation between replicate plots) and cover of sedges, grasses and mosses.

Site	$Mg\,C\,ha^{-1}\,a^{-1}$	$kg\,N\,ha^{-1}\,a^{-1}$	Sedge cover [%][a]	Grass cover [%][a]	Moss cover [%][a]
C_{med} W_{39}	2.3 ± 005	95 ± 3	10	70	0
C_{low} W_{29}	2.9 ± 0.14	138 ± 7	0	90	0
C_{low} W_{14}	1.7 ± 0.28	68 ± 10	55	15	0
C_{high} W_{11}	0.28 ± 0.03	8 ± 1	35	25	95
C_{high} W_{22}	0.57 ± 0.04	19 ± 2	15	65	65
C_{high} W_{17}	0.39 ± 0.02	14 ± 1	50	20	75

[a] Cover values are indicated to 5 % exactly.

BGD
10, 11283–11317, 2013

Table 3. Annual fluxes of NEE, Reco and GPP, CH_4 and N_2O (1 June 2011 to 1 June 2012; annual flux ± one stand ard deviation).

Site	NEE [$Mg\,C\,ha^{-1}\,a^{-1}$]	Reco [$Mg\,C\,ha^{-1}\,a^{-1}$]	GPP [$Mg\,C\,ha^{-1}\,a^{-1}$]	CH_4 [$Mg\,C\,ha^{-1}\,a^{-1}$]	N_2O [$kg\,N\,ha^{-1}\,a^{-1}$]
C_{med} W_{39}	6.3 ± 0.4	18.6 ± 0.4	−12.3 ± 0.2	0.002 ± 0.001	0.02 ± 0.12
C_{low} W_{29}	5.7 ± 0.4	19.7 ± 0.4	−14.0 ± 0.3	0.001 ± 0.001	0.05 ± 0.15
C_{low} W_{14}	4.9 ± 0.3	15.4 ± 0.3	−10.5 ± 0.2	0.021 ± 0.002	−0.27 ± 0.14
C_{high} W_{11}	3.0 ± 0.3	8.6 ± 0.3	−5.6 ± 0.2	0.028 ± 0.001	−0.10 ± 0.28
C_{high} W_{22}	3.9 ± 0.3	10.4 ± 0.3	−6.5 ± 0.2	0.005 ± 0.001	−0.03 ± 0.17
C_{high} W_{17}	3.2 ± 0.4	9.6 ± 0.3	−6.5 ± 0.2	0.030 ± 0.003	−0.09 ± 0.17

BGD
10, 11283–11317, 2013

Table 4. Global warming potential for a time horizon of 100 yr (GWP100) of Net C balance (NEE plus harvest), CH_4 and N_2O and total GHG balance (annual flux ± one stand ard deviation; IPCC 2007).

Site	GWP100-C balance [$Mg\,CO_2-C\,eq.\,ha^{-1}\,a^{-1}$]	GWP100-CH_4 [$Mg\,CO_2-C\,eq.\,ha^{-1}\,a^{-1}$]	GWP100-N_2O [$Mg\,CO_2-C\,eq.\,ha^{-1}\,a^{-1}$]	GWP100-GHG balance [$Mg\,CO_2-C\,eq.\,ha^{-1}\,a^{-1}$]
C_{med} W_{39}	8.5 ± 0.40	0.012 ± 0.005	0.003 ± 0.017	8.5 ± 0.40
C_{low} W_{29}	8.6 ± 0.42	0.008 ± 0.006	0.006 ± 0.020	8.7 ± 0.42
C_{low} W_{14}	6.6 ± 0.41	0.158 ± 0.012	−0.037 ± 0.018	6.7 ± 0.41
C_{high} W_{11}	3.3 ± 0.30	0.205 ± 0.009	−0.013 ± 0.037	3.5 ± 0.30
C_{high} W_{22}	4.5 ± 0.30	0.040 ± 0.004	−0.005 ± 0.023	4.5 ± 0.30
C_{high} W_{17}	3.5 ± 0.40	0.221 ± 0.021	−0.013 ± 0.023	3.8 ± 0.40

BGD
10, 11283–11317, 2013

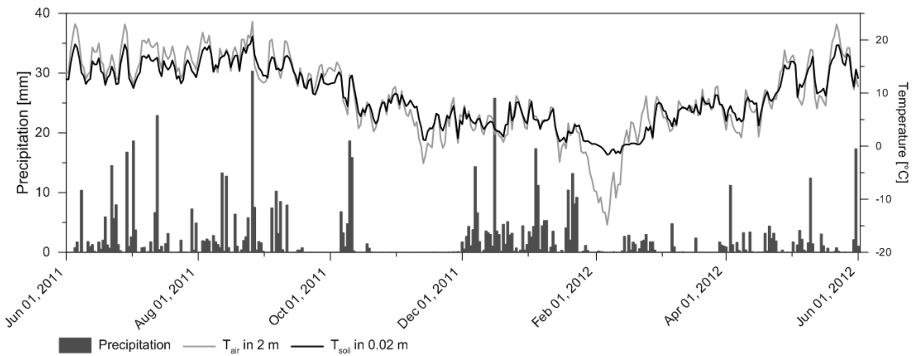

Fig. 1. Time series of precipitation, air, and 2 cm soil temperature at meteorological station.

BGD
10, 11283–11317, 2013

High greenhouse gas fluxes from grassland on histic gleysol

K. Leiber-Sauheitl et al.

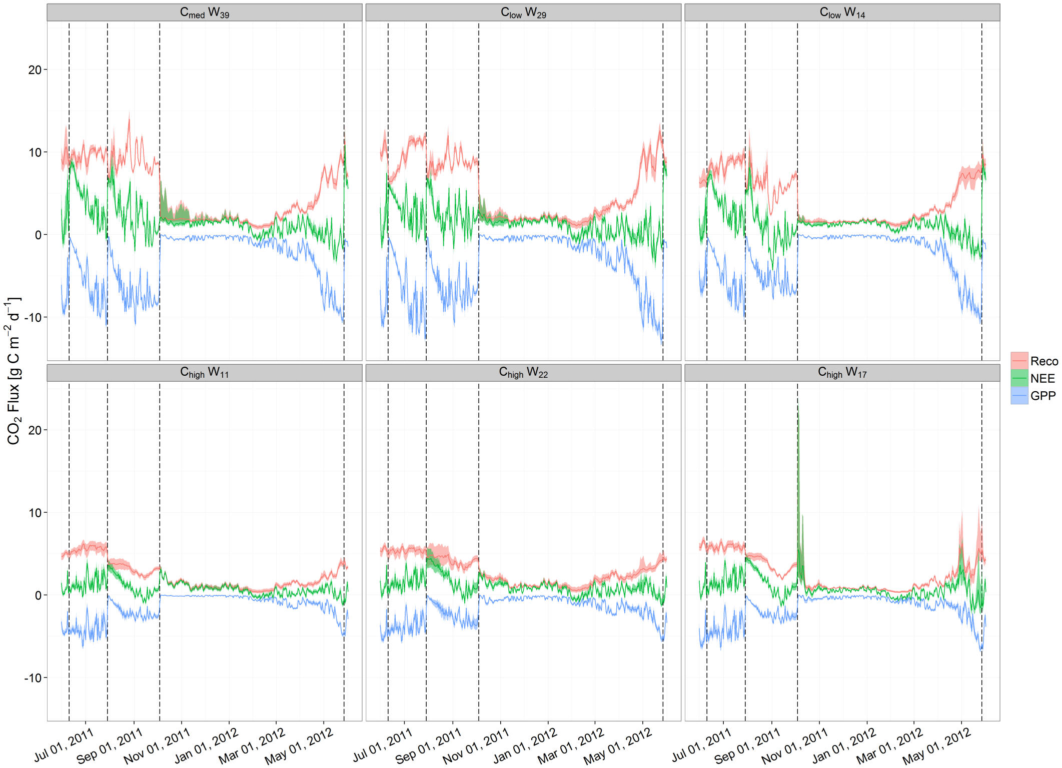

Fig. 2. Time series of daily CO_2 fluxes [$g\,C\,m^{-2}\,d^{-1}$] at each site (1 June 2011–1 June 2012). Depicted are modeled fluxes and 95 % confidence band. Dashed lines indicate grazing and mulching events.

BGD
10, 11283–11317, 2013

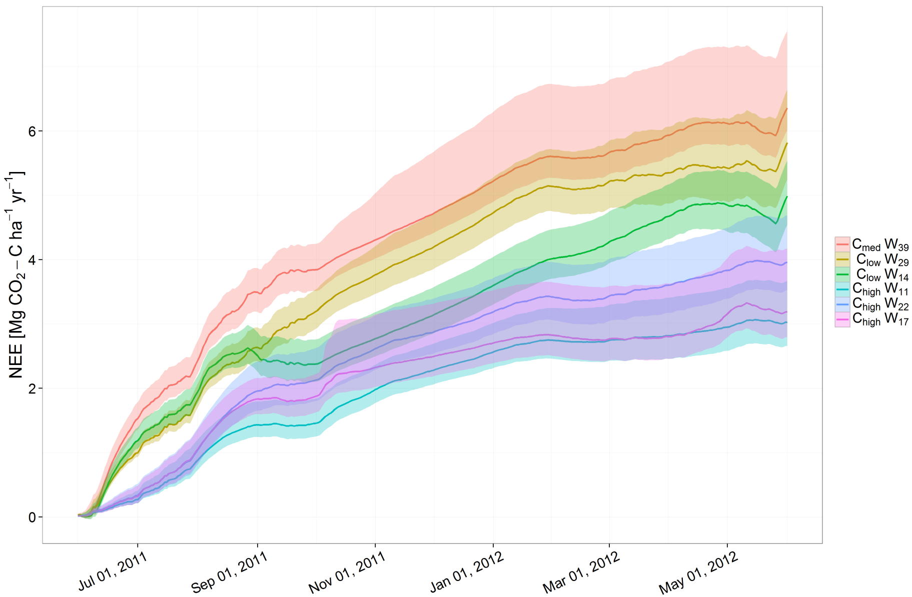

Fig. 3. Cumulative sum of NEE of each site in the Grosses Moor (1 June 2011 to 1 June 2012). Continuous line: modeled NEE values, colored space around continuous line: 95 % confidence interval.

BGD
10, 11283–11317, 2013

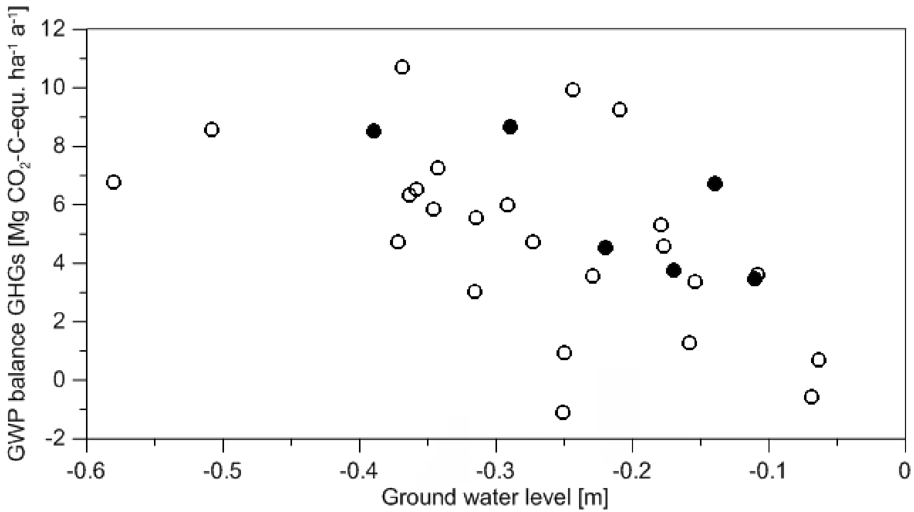

Fig. 4. Annual GHG balances vs. water table level of shallow peat sites in the Grosses Moor (filled circles) and several deep peat grassland sites (open circles) in Germany (Drösler et al., 2013).

BGD
10, 11283–11317, 2013

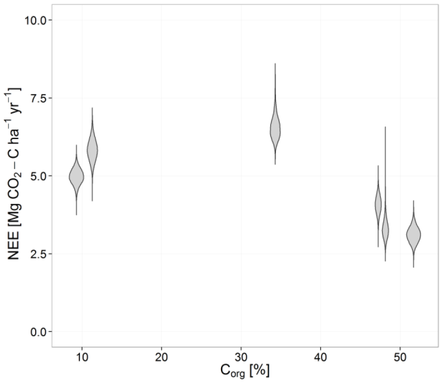

A

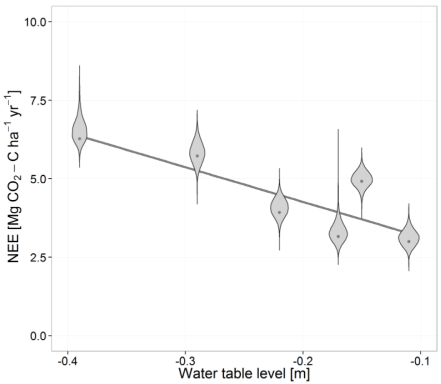

B

Fig. 5. Violin plots of NEE emissions vs. C_{org} (**A**; R^2 = 0.49, p = 0.121) and NEE emissions vs. water table level (**B**; R^2 = 0.71, p = 0.035). Violins **(A, B)**: distribution of all simulated aggregated annual NEE sums of each site; points **(B)**: modeled annual NEE of each site, used as basis for linear regression.

BGD
10, 11283–11317, 2013

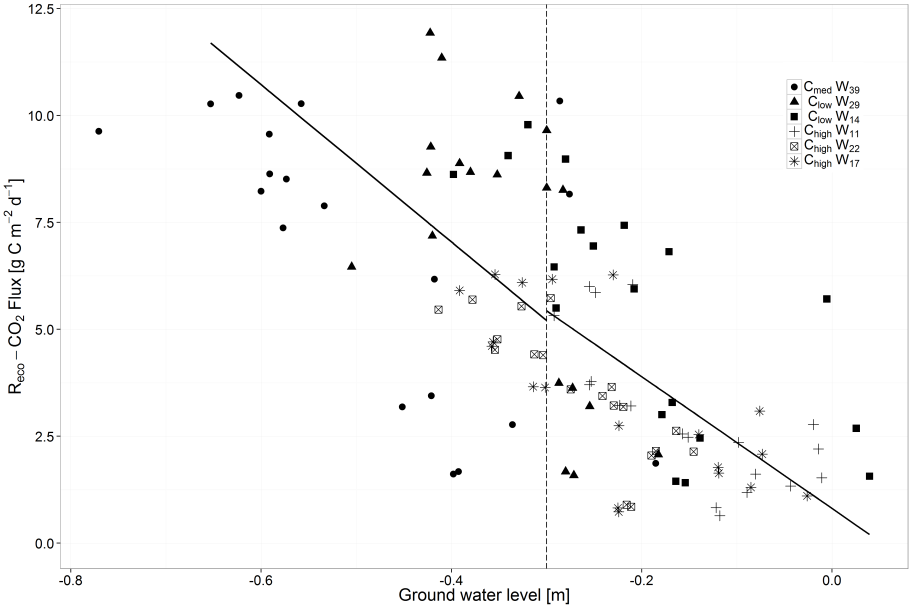

Fig. 6. Ground water levels [m] vs. R_{eco}-CO_2 flux [g C m^{-2} d^{-1}] on the campaign dates for all six sites. Dotted vertical line: border of peat horizon; continuous line: population mean prediction from the linear mixed effects model for all sites; a fixed effect was used to distinguish water levels below the peat horizon (−0.8 to −0.3 m) and within the peat horizon (−0.3 to +0.1 m).

BGD
10, 11283–11317, 2013